THE ASTROPHYSICAL JOURNAL, 267:528–534, 1983 April 15

H I OBSERVATIONS OF THE HIGH-VELOCITY SYSTEM IN NGC 1275

J. H. VAN GORKOM[1] AND R. D. EKERS[1]
Kapteyn Astronomical Institute, Groningen, The Netherlands
Received 1981 October 5; accepted 1982 October 12

ABSTRACT

An attempt to detect H I emission from the high-velocity system in the Seyfert galaxy NGC 1275 (Perseus A) is presented. The data were obtained with the Westerbork Synthesis Radio Telescope using a special calibration procedure to achieve high spectral dynamic range. The new upper limit of $2.4 \times 10^9\ M_\odot$ for the total H I mass in this system makes it unlikely that it is a very late-type galaxy, but the limit is still not low enough to exclude galaxies of type Sc or earlier.

A tentative detection of a new weak broad absorption feature is reported, and the implications of an observed 30% increase in the intensity of the strong absorption feature are discussed.

Subject headings: galaxies: individual — galaxies: Seyfert — radio sources: 21 cm radiation

I. INTRODUCTION

De Young, Roberts, and Saslaw (1973) detected H I absorption in NGC 1275 at a velocity of 8120 km s^{-1}. This is 3000 km s^{-1} larger than the systemic velocity of NGC 1275 and is the same velocity as that of the enigmatic system of gas filaments extending 40″ from the nucleus. Ekers, van der Hulst, and Miley (1976) established that the H I absorption is occurring against the nucleus (< 0.″05 component) of NGC 1275. They also placed an upper limit of $10^{10}\ M_\odot$ for the total mass of H I associated with the 8200 km s^{-1} system; however, their velocity coverage was only 290 km s^{-1}, so features broader than about 200 km s^{-1} would not have been detected. Rubin *et al.* (1977) and Kent and Sargent (1979) published new spectroscopic and plate material showing that there is a smooth variation in velocity of 300 km s^{-1} across the high-velocity region. They suggest that this is consistent with a picture of a rotating late-type galaxy seen almost edge-on. With the new optical data and the replacement of the 80 channel filter-spectrometer by a digital cross-correlator at Westerbork, it seemed worthwhile to make a new attempt to detect H I emission. The digital cross-correlator is more suitable for this type of experiment because it has a broader bandwidth and has a much better channel to channel stability than the filterspectrometer.

II. OBSERVATIONS AND CALIBRATION

The observations were obtained with the Westerbork Synthesis Radio Telescope using the digital line back-end in a 1 bit mode and an analog delay system (Bos, Raimond, and van Someren Greve 1981). Initially, a total bandwidth of 10 MHz (2200 km s^{-1}) was used to cover the full velocity range of the optical emission lines. Following a tentative detection of a new weak absorption feature described in § III*b*, another set of observations was made with higher velocity resolution and a 2.5 MHz total bandwidth. The instrumental parameters of both observations are given in Table 1.

The continuum flux density of NGC 1275 is very high compared with the line emission, so special calibration techniques were developed to obtain high spectral dynamic range. The source was observed twice for 12 hours, once centered on the H I frequency and once at a 10 MHz higher frequency. Both these observations were calibrated by observing 3C 295 for 3 hours before and 3 hours after NGC 1275. The observation at the displaced frequency was then used to self-calibrate NGC 1275, as described in the next section.

a) The 10 MHz Bandwidth Observation

The average gain and phase for each velocity channel for each interferometer were determined by the observation of 3C 295 (1383 MHz flux density assumed to be 22 Jy). The relative phases of different velocity channels vary slightly during a 12 hour period. Since this effect is mainly due to dispersion in the delay cables, it is proportional to both the frequency offset from the center of the band and the length of the delay cables. This chromatic phase error causes any sources in the maps appear to shift slightly in position as a function of frequency. Since the relative offsets in frequency and the inserted delays are identical for the two observations, we could remove this effect by complex dividing the visibility data at the line frequency by the data at the displaced frequency (point by point in the UV plane). A side

[1]Present address: NRAO, Socorro, NM. The National Radio Astronomy Observatory is operated by Associated Universities, Inc., under contract with the National Science Foundation.

TABLE 1

INSTRUMENTAL PARAMETERS

Parameter	Observation 1	Observation 2
Field center α (1950)	$3^h16^m29^s.6$	$3^h16^m29^s.6$
Field center δ (1950)	41°19′52″.0	41°19′52″.0
Observation dates	1978 March 19, 20	1979 January 19, 20
T_{sys}	90 K	90 K
Number of spacings	40	20
Shortest spacing (m)	36	36
Spacing interval (m)	36	Alternating 36, 108
Longest spacing (m)	1440	1368
Primary beam (FWHP) (arc min)	36	36
Radius of first grating ring (arc min)	20×30 ($\alpha\times\delta$)	5×7.6 ($\alpha\times\delta$)
Synthesized beam (FWHP) (arc sec)	22×33 ($\alpha\times\delta$)	26×36 ($\alpha\times\delta$)
Total bandwidth (MHz)	10	2.5
No. of velocity channels	64	128
Velocity range ($V_{Hel} = c\Delta\lambda/\lambda_0$) (km s^{-1})	7481–9644	7890–8421
Channel separation (km s^{-1})	35	4.35
Velocity resolution (km s^{-1})	42	5.2
Dynamic range (dB)	34	Noise limited
Rms noise (mJy per beam)	2.3[a]	6.5[b]

[a] Theoretical noise; observation is limited by dynamic range.
[b] Observed after Hanning smoothing.

effect of this procedure is the removal of the very weak extended continuum emission around NGC 1275. This occurs because the complex visibilities are normalized with respect to their value at an adjacent frequency. The resulting maps can be considered as being made with an antenna pattern that has slightly lower weights at the shorter baselines. This has no important consequences in any of the following discussion.

The strong absorption feature detected by de Young, Roberts, and Saslaw (1973) was unresolved with this velocity resolution, and consequently the channel maps were seriously distorted by the velocity sidelobes from this feature. To remove these sidelobes, we subtracted the expected response of a point (in both frequency and space) source. The frequency response was assumed to be a sinc function, and the mean of all channel maps was used for the spatial response.

Finally a mean "continuum," formed by averaging all the channel maps, was subtracted from all channel maps.

The resulting line maps showed very regular frequency dependent rings around NGC 1275. The rings had a maximum amplitude of 0.3% of the continuum peak intensity and were probably due to the slight scale change in the synthesized beam across the frequency band. Since they were very regular, they were removed by fitting linear baselines to the profiles at each position in the map. The spectral dynamic range (rms/peak) finally achieved was 34 dB (0.04%).

b) The 2.5 MHz Bandwidth Observation

The much smaller bandwidth and a better on-line correction for dispersion effects removed the necessity for the frequency shift and self-calibration in these data. Also, the velocity resolution was a factor of 8 higher which was sufficient to resolve the strong absorption feature and reduce the frequency sidelobes sufficiently to alleviate the need to subtract the absorption line.

To clarify the nature of other possible frequency dependent effects, we corrected each channel map separately for the small change in scale of the synthesized beam across the band using the following procedure. First, a mean continuum was formed by averaging all the line-free channel maps. Then 20 point components representing the mean continuum map were found using the CLEAN algorithm (Högbom 1974; Schwarz 1978). These *same* components were subtracted from all channel maps using the appropriate synthesized beam for each channel. This removed the major part of the continuum emission with the correct beam width and without introducing additional noise. The residual mean continuum was weak enough to be subtracted from all channel maps without this beam correction. The resulting line maps showed a slope in intensity that was linear with frequency. Since the slope was proportional to the amplitude in the continuum map and reached a maximum of 0.3% at the edges of the band, it could be explained by the spectral index difference between 3C 295 and NGC 1275. Finally, Hanning smoothed profiles were formed, and a linear baseline was removed at each point in the map.

III. RESULTS

a) H I Emission

Optical emission lines from the high-velocity system have been detected over an area of $\sim 60''\times20''$ ($\alpha\times\delta$)

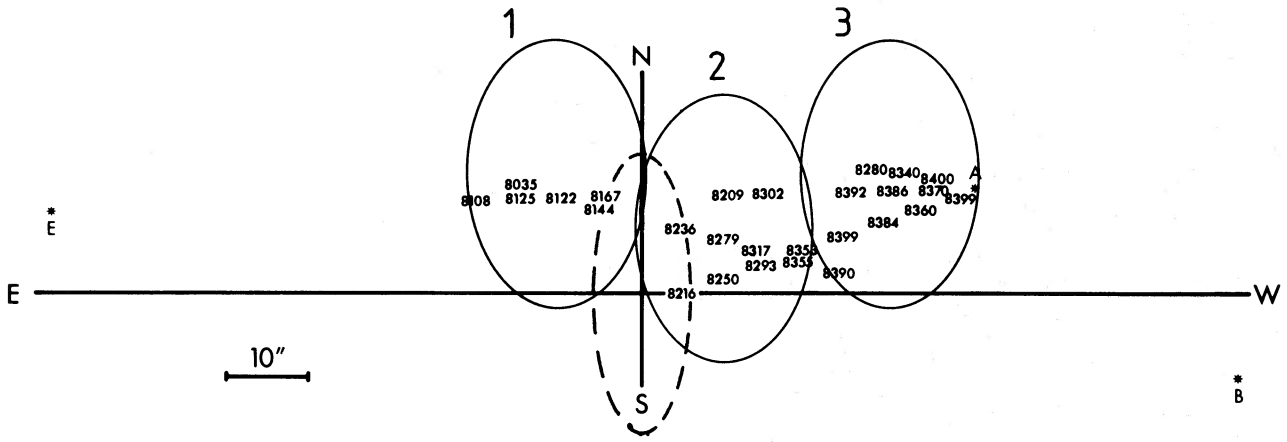

FIG. 1.—NGC 1275 high velocity system. The positions and the synthesized beam width (HPBW) for these observations are indicated by the three filled ellipses. These are superposed on the velocity field for the high velocity system as measured by Rubin *et al.* 1977. The dashed ellipse indicates the intermediate size continuum component (Miley and Perola 1975). The nucleus of the underlying galaxy is located at the origin.

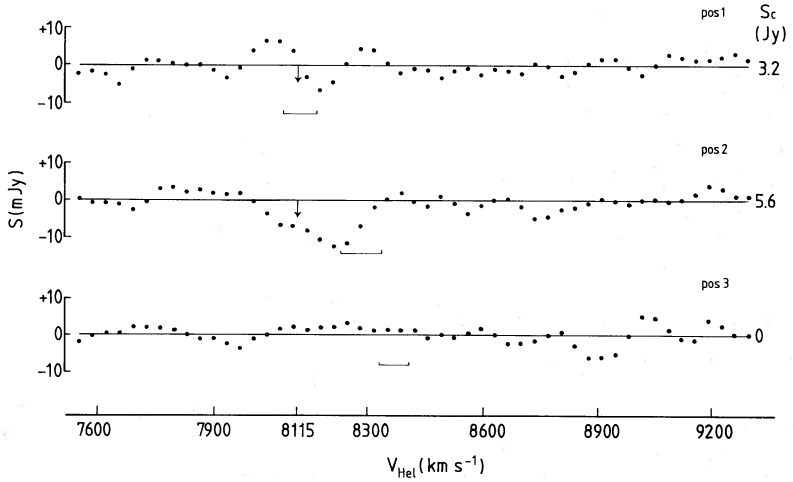

FIG. 2.—The broad-band spectra at the three positions shown in Fig. 1. The strong absorption feature has been subtracted; the small arrow indicates its position in the band. The spectra are Hanning smoothed, and a linear baseline has been removed. The mean optical velocity and its dispersion ($\pm 1\ \sigma$) are indicated below each spectrum. The continuum flux density at each position is indicated at the right.

(Rubin *et al.* 1977; Kent and Sargent 1979). With our resolution of $22'' \times 33''$ we can get three independent measurements in this area. In Figure 1 we indicate these positions superposed on the velocity field of Rubin *et al.* The mean optical velocities are 8116 ± 45, 8281 ± 51, and 8371 ± 38 km s^{-1} at position 1, 2, and 3, respectively. The broad-band H I spectra at these three positions and the optical velocity ranges are shown in Figure 2. No emission can be seen in the optical velocity range; however, there is some indication of absorption at these velocities in positions 1 and 2 where there is strong continuum emission. Since these two spectra cannot be used to derive an upper limit for H I emission, we assume that the H I is smoothly distributed over the same area as the optical lines and only use position 3. The profile at position 3 was smoothed to a velocity resolution of 105 km s^{-1} (three channels), corresponding to the optical velocity range over our beam at this position. The rms is then $\sigma = 1.9$ mJy per 105 km s^{-1}.

Using $M_{\rm H\,I} = 2.36 \times 10^5\ D^2$ (Mpc) S(Jy) Δv(km s^{-1}) [$M_\odot$] and taking $D = 75$ Mpc ($H_0 = 75$ km s^{-1} Mpc^{-1}) and using for S a 3 σ limit of 5.7 mJy gives:

$$M_{\rm H\,I} < 0.8 \times 10^9\ M_\odot$$

at position 3. Assuming this limit applies over the total area of the optical emission we get:

$$M_{\rm H\,I} < 2.4 \times 10^9\ M_\odot.$$

It should be noted that the radio spectra just south of the nucleus, where there is no optical high-velocity emission, look essentially similar to the one in position 3. So there is no reason to believe that the H I is distributed differently from the ionized gas.

b) H I *Absorption, A Very Weak Broad Feature*

In Figure 2 we noted that in positions 1 and 2 there is a dip in the profile at a velocity close to the optical range. This could be absorption against the intermediate size (30″) continuum component (Miley and Perola 1975). Even though no similar features are seen in the spectra in the symmetric positions to the south of the nucleus, we were not completely sure that it could not be an artifact resulting from the subtraction of the strong absorption feature. Consequently, a second set of observations was undertaken with sufficient velocity resolution to resolve the strong absorption feature and just enough total bandwidth to cover the absorption dip. In Figure 3 we plot the results of the new observations at seven positions at and around the nucleus. At three of the positions (−10, +15; −10, 0; and 0, 0) absorption can be seen, this can be compared with the low resolution observations also plotted in Figure 3 (*dots*) which show absorption at the same positions. Table 2 summarizes the parameters of the broad absorption feature in both observations. The mean of the three profiles has a depth of ~12 mJy and a width of 185 km s^{-1}. This is below the sensitivity limit of the observations by de Young, Roberts, and Saslaw (1973), but the feature might be seen at the 1× rms level in the data of Ekers, van der Hulst, and Miley (1976). Since we do not see absorption in the profile half a beamwidth south of the nucleus, this absorption cannot be against the central source. The central velocity of the feature is less than the mean optical velocity at all positions, but there is partial overlap between the H I and optical velocities. Since the continuum is not uniform over our beam, such a difference in velocity can be expected.

There are two extended continuum components (Miley and Perola 1975) against which absorption could occur: (1) an intermediate size component (30″×15″, ~2 Jy) for which the structure is not well established, but is possibly elongated to the south (position angle 170°), and (2) a halo component (3′×4′, ~2 Jy) and roughly elongated in the same direction centered at NGC 1275. If we assume that the absorbing cloud homogeneously covers either component, a lower limit for the column

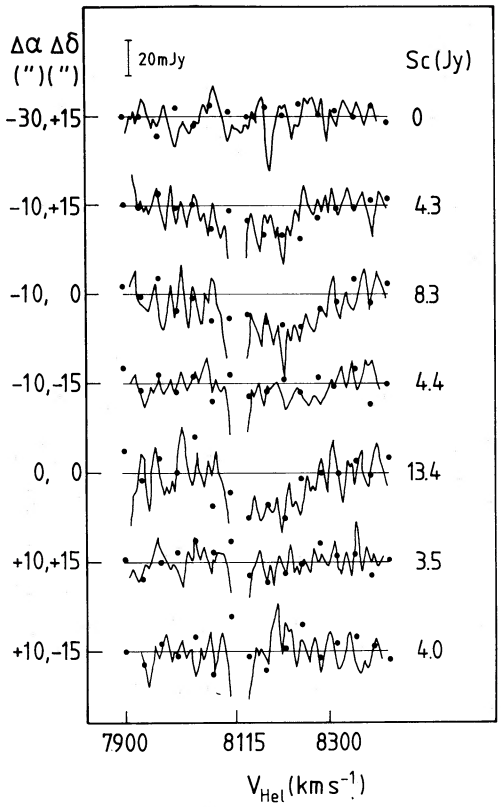

FIG. 3.—Seven profiles near the nucleus of NGC 1275. On the left the relative offset from the nucleus is indicated; on the right the continuum intensity. The solid lines are the high resolution spectra (Hanning smoothed). The dots are broad-band spectra from which the strong absorption feature has been subtracted. In both spectra a linear baseline has been removed.

TABLE 2

PARAMETERS OF THE WEAK ABSORPTION FEATURE

	VALUE							
	10 MHz Bandwidth				2.5 MHz Bandwidth			
Δα, Δδ (arcsec)	S_{cont} (Jy)	S_{abs} (mJy)	ΔV (km s^{-1})	V_c (km s^{-1})	S_{cont} (Jy)	S_{abs} (mJy)	ΔV (km s^{-1})	V_c (km s^{-1})
−10,15 ...	4.2	10±2[a]	140	8175±40	4.3	10±2[a]	154	8173±35
−10,0	7.1	10	245	8158	8.3	12	223	8194
0,0	12.6	16	175	8141	13.4	12	189	8183

[a] Error estimates are based on the assumption that the noise is random from channel to channel.

density can be derived, using

$$N_{\rm H\,I} = 1.82 \times 10^{18}\, T_s({\rm K})\, \tau \Delta v\,({\rm km\ s^{-1}})\ [{\rm cm^{-2}}].$$

For the intermediate component, assuming that 1 Jy is covered by the cloud, this gives:

$$\tau = 0.01 \quad \text{and} \quad N_{\rm H\,I} > 4 \times 10^{18}\, T_s\ {\rm cm^{-2}}.$$

For the halo we assume that 2% is covered by our beam, giving

$$\tau = 0.44 \quad \text{and} \quad N_{\rm H\,I} > 1.5 \times 10^{20}\, T_s\ {\rm cm^{-2}}.$$

However, our failure to detect H I emission provides an upper limit on the column density, since $N_{\rm H\,I} = 1.8 \times 10^{-18}\, T_b \Delta v$. We use our 3 σ upper limit of 5.7 mJy, which corresponds to a limit in brightness temperature of 4.6 K (assuming the whole beam is filled), and we take $\Delta v = 185$ km s^{-1}, the velocity range found by Kent and Sargent (1979), and also the width of the absorption line, to derive $N_{\rm H\,I} < 10^{21}$ cm^{-2}. This limit clearly rules out absorption against the halo for any reasonable spin temperature. For the intermediate component we can combine the two limits to give a limit on spin temperature of $T_s < 250$ K.

c) *The Depth of the Strong Absorption Line*

Ekers, van der Hulst, and Miley (1976) have pointed out that although the flux density of the compact component at 1.4 GHz had increased by 15%, the optical depth in the strong feature had remained constant. Since then, the flux density has gone up by more than 50%, so we can investigate changes in optical depth more easily. The available data are taken with very different velocity resolution, so we compare only the integrated optical depth, $\int \tau_L\, dv$, taking the integration limits from ~ 8100 to ~ 8135 km s^{-1}. In Table 3, Westerbork data on the continuum emission of the compact component are given and the relative absorption as measured by a variety of instruments. Even allowing for uncertainties introduced by the different calibration and velocity resolution of these observations, it appears that the relative absorption has increased by roughly 30%.

Two possible explanations are (1) the continuum source changed position with respect to the clouds, or (2) only part of the continuum flux density of the compact component is varying. Explanation (1) is unlikely since superluminal velocities are required and the VLBI maps of Matveyenko *et al.* (1980) show no evidence of relative motions of the components. Furthermore, the shape of the absorption profile of the two stronger components has remained constant, strongly suggesting that the same clouds are absorbing. To evaluate the second possibility we need to know the structure of the compact source at 21 cm. Romney (1979) found that it consists of two concentric components with sizes of 5×8 milli-arcsec, and 9×25 milli-arcsec. He also showed that the two stronger features absorb against the smaller component. If we assume that the optical depth has remained constant and that the continuum has one constant and one variable component, we find a flux density of 4.4 Jy for the constant component and a peak optical depth of 0.4 against the variable component. Since this is a reasonable value for an interstellar cloud, we consider this the more likely explanation.

TABLE 3

VARIABILITY OF COMPACT SOURCE AND RELATIVE ABSORPTION

Date	Frequency (MHz)	Flux Density[a] (Jy)	$\int \tau_L dv$ (km s^{-1})
1971 Jun 5	1.415	7.3 ± 0.1	$1.7 \pm .2$[b]
1974 Aug 11 ...	1.383	8.6 ± 0.1	...
1974 Oct 10 ...	1.415	8.7 ± 0.1	...
1974 Nov 15 ...	1.383	8.6 ± 0.1	1.7[c]
1978 Mar 19 ...	1.381	11.3 ± 0.1	$2.25 \pm .05$
1979 Jan 19 ...	1.383	12.2 ± 0.1	$2.19 \pm .05$
1979 Dec 16 ...	1.383	(12.4 ± 0.1)[d,e]	$2.11 \pm .06$[d]

[a] Flux densities as observed with the WSRT.

[b] From de Young *et al.* 1973 observed with 140 foot (42.6 m). Assumed flux density of compact component is 7.3 Jy (Wilkinson 1972). Error is mainly due to uncertainty in calibration.

[c] From Ekers *et al.* 1976. Profile is undersampled.

[d] From J. M. van der Hulst, A. D. Haschick, and P. C. Crane (private communication), observed with VLA. Flux density of compact component is 12.4 ± 0.2 Jy.

[e] The VLA has different spatial resolution, so this value may not be directly comparable to the others in the table.

IV. DISCUSSION

Support for the hypothesis that the high velocity system is an intervening late-type spiral galaxy have been obtained by Rubin *et al.* (1977) and by Kent and Sargent (1979). The main objections to this hypothesis are the low probability of such a chance superposition and the unusual morphology of the intervening galaxy. The absence of any nucleus (Oort 1976) or stellar continuum (Burbidge, Smith, and Burbidge 1978) and the presence of many emission regions and dust suggest a very late-type spiral or irregular galaxy, but its diameter is similar to that of a normal spiral.

We have improved the upper limit on the total H I mass of the hypothetical intervening system by a factor of 4 compared to that of Ekers, van der Hulst, and Miley (1976) and have sufficient velocity range to make this a definite limit. This limit can be compared with the H I mass expected for a late-type galaxy. Following Shostak (1978), we define a total mass as:

$$M_T = 2.45 \times 10^4\, A_0 \Delta V_0^2\, [M_\odot],$$

TABLE 4

HYDROGEN MASS IN LATE-TYPE GALAXIES

VARIABLE	TYPE					
	4(Sbc)	5(Sc)	6(Scd)	7(Sd)	9(Sm)	10(Im)
Total no. of galaxies	20	22	27	6	1	6
Percentage with $\frac{M_{\rm H\,I}}{M_T} < 0.05$ ...	60	59	26	33	0	0

where A_0 is the photometric diameter (kpc) and ΔV_0 is the hydrogen profile width corrected for inclination $\Delta V/\sin(i)$ km s^{-1}. Taking $A_0 = 22$ kpc and $\Delta V/\sin(i) = 300$ km s^{-1}, we find $M_T = 4.8\times10^{10}\ M_\odot$ and $M_{\rm H\,I}/M_T < 0.05$. In Table 4 we give the percentage of galaxies with $M_{\rm H\,I}/M_T < 0.05$ for a given type taken from Shostak's sample. Galaxies that are possibly confused or have inclination $< 30°$ or are of type P(eculiar) or B(arred) are excluded. From Table 4 it appears that it is not very likely that the high velocity system is a very late-type galaxy, as is preferred by Kent and Sargent (1979), but the limit is still not low enough to exclude galaxies of type Sc or earlier. Our limit is rather low compared with the observed reddening. Rubin *et al.* (1977) have shown that the low-velocity system is being obscured by the high-velocity system. The observed reddening toward the low-velocity system is $E(B-V) = 0.43$ (Kent and Sargent 1979) and using a galactic gas-to-dust ratio (Knapp and Kerr 1974), this would imply $N_{\rm H\,I} = 2\times10^{21}$ cm^{-2}, which is a factor 4 more than the upper limit we obtain. This discrepancy can be explained if the dust distribution is more patchy than the H I distribution.

The tentative detection of a broad absorption feature is in agreement with the intervening galaxy hypothesis. If the strong absorption feature is caused by an interstellar cloud, one would expect to pick up many of these clouds against a more extended continuum source, and they would have roughly the observed spread in velocities.

Finally, we can make some remarks on the minimum distance of the H I from the nucleus of NGC 1275. The ultraviolet radiation from the nonthermal continuum source (Shields and Oke 1975) or the extended X-ray source (Kent and Sargent 1979) could ionize H I clouds out to large distances (> 65 kpc). However, the H I could be shielded against radiation at these wavelengths. We now consider the effect of the 21 cm continuum radiation on the spin temperature. In this case shielding would only be possible if the densities were extremely high, and the results of both Romney (1979) and the present paper make this very unlikely. Normally the spin temperature of the H I is coupled to the gas kinetic temperature via collisions. Near a strong radio source, however, (de)excitation by 21 cm photons may play a role. If we neglect the effect of Lyα excitation, the appropriate expression for the spin temperature is (Bahcall and Ekers 1969):

$$T_s = (T_R + y_c T_k)/(1 + y_c),$$

where T_R is the continuum brightness temperature (averaged over all solid angles) and y_c is proportional to the collisional deexcitation rate. Following Bahcall and Ekers we find that for NGC 1275

$$T_R \sim 7.9\times10^4\, r^{-2}\ [\rm K]$$

at a distance r (kpc) from the source. If we assume standard H I conditions ($n_{\rm H} = 100$ cm^{-3}, $T_k = 100$ K), our upper limit of $T_s < 250$ K implies that $T_R < 6\times105$ K and hence $r > 400$ pc. The recent increase in relative absorption of the strong feature gives a slightly better limit. The assumption of one constant and one variable component provides a lower limit to the amount of change in flux density of 3 Jy to 8 Jy. At a distance of 500 pc, this increase would cause a decrease in optical depth of 30%, resulting in a constant relative absorption against the total source, whereas an increase of 30% is seen (§ III*c*). We can conclude that the H I has to be further away than about 1 kpc.

We thank S. Shostak for helpful discussions about the H I emission and G. Swarup, J. Romney, W. M. Goss, and J. M. van der Hulst for stimulating discussions. J. M. van der Hulst also provided VLA results prior to publication. The comments from the referee have been very useful.

We thank the staff of the Netherlands Foundation for Radio Astronomy for their aid in obtaining the data. The data reduction was done with the facilities of the University of Groningen Computing Centre. J. H. v. G. acknowledges financial support from the Netherlands Organization for the Advancement of Pure Research (Z. W. O.). The WSRT is operated by the Netherlands Foundation for Radio Astronomy, which is financially supported by Z. W. O.

REFERENCES

Bahcall, J. N., and Ekers, R. D. 1969, *Ap. J.*, **157**, 1055.
Bos, A., Raimond, E., and van Someren Greve, H. W. 1981, *Astr. Ap.*, **98**, 251.
Burbidge, E. M., Smith, H. E., and Burbidge, G. R. 1978, *Ap. J.*, **219**, 400.
de Young, D. S., Roberts, M. S., and Saslaw, W. C. 1973, *Ap. J.*, **185**, 809.
Ekers, R. D., van der Hulst, J. M., and Miley, G. K. 1976, *Nature*, **262**, 369.
Högbom, J. A. 1974, *Astr. Ap. Suppl.*, **15**, 417.
Kent, S. M., and Sargent, W. L. W. 1979, *Ap. J.*, **230**, 667.
Knapp, G. R., and Kerr, F. J. 1974, *Astr. Ap.*, **35**, 361.
Matveyenko, L. I., *et al.* 1980, *Soviet Astr. Letters*, **6**, 42.
Miley, G. K., and Perola, G. C. 1975, *Astr. Ap.*, **45**, 223.
Oort, J. H. 1976, Pub. *A.S.P.*, **88**, 591.
Romney, J. D. M. 1979, Ph.D. thesis, California Institute of Technology.
Rubin, V. C., Ford, W. K., Jr., Peterson, C. J., and Oort, J. H. 1977, *Ap. J.*, **211**, 693.
Schwarz, U. J. 1978, *Astr. Ap.*, **65**, 345.
Shields, G. A., and Oke, J. B. 1975, *Pub. A.S.P.*, **87**, 879.
Shostak, G. S. 1978, *Astr. Ap.*, **68**, 321.
Wilkinson, P. N. 1972, *M.N.R.A.S.*, **160**, 305.

R. D. EKERS and J. H. VAN GORKOM: National Radio Astronomy Observatory, P.O. Box 0, Socorro, New Mexico 87801